AUT Journal of Mechanical Engineering

AUT J. Mech. Eng., 8(1) (2024) 31-42
DOI: 10.22060/ajme.2024.23182.6110

Buckling Analysis of the Composite Sandwich Cylindrical Shell Integrated with Auxetic Metamaterial Core

Korosh Khorshidi *, Saboor Savvafi, Sadegh Zobeid

Department of Mechanical Engineering, Arak University, Arak, Iran

ABSTRACT: This study investigated the effect of an auxetic structure, positioned as the central layer in a three-layered cylindrical shell, on its buckling behavior. The material for all three layers is aluminum. The covers are assumed isotropic. Axial and static loads are modeled as pressure on the shell's surface. In this study, modified shear deformation theory and Galerkin's numerical solution method were used, and the effect of the presence of an auxetic core on the buckling behavior of a three-layered cylindrical shell was investigated. The assumed structure for the auxetic cell was a 2D Re-entrant honeycomb. Finally, we explore how the length-to-radius ratio, core thickness-to-total thickness ratio, and cell angle of the auxetic structure impact the system's stability, presenting the results. The distinguishing feature of the current work compared to previous studies lies in its mathematical approach. We present the system's equations as comprehensively as possible. Finally, the effect of the length-to-radius ratio, the auxetic layer's thickness relative to the whole shell's thickness, and the cell angle's size on the buckling load were investigated. In short, with the increase of both ratios, the amount of load required for buckling decreases, or in other words, system stability is reduced. Also, the size of the cell angle has little effect on the system's stability.

Review History:

Received: May, 12, 2024
Revised: Jun. 09, 2024
Accepted: Jul. 13, 2024
Available Online: Jul. 18, 2024

Keywords:

Buckling
Composite Cylindrical Shell
Auxetic Structure
High Order Shear Deformation Theory (HSTD)

1- Introduction

The study of buckling in shells is crucial in structural mechanics. Buckling often leads to structural failure and can occur without prominent warning, making it particularly important for shell structures. Understanding buckling behavior helps estimate critical loads at which shells may buckle, preventing catastrophic collapse. Additionally, comprehensive analyses of buckling and strength provide valuable information about structural deformation and verify load values. Whether it is analyzing cylindrical panels, viscoelastic spherical shells, or silos, studying buckling ensures safer and more reliable structures.

Cylindrical shells find widespread application across various industries, including oil and gas, marine, aerospace, and construction. Simultaneously, scientists and researchers continually strive to enhance material properties and characteristics. Advances in manufacturing technology have enabled the production and presentation of a wide range of materials. Among these, auxetic materials-part of the metamaterial family-stand out due to their unique features [1]. As a result, they have garnered interest in using them in diverse structural applications. The focus of this study is to investigate the buckling behavior of a three-layered cylindrical shell that incorporates an auxetic structure in its central layer.

*Corresponding author's email: k-khorshidi@araku.ac.ir

Unlike ordinary materials, auxetic materials expand and contract in the direction perpendicular to the applied load axis when subjected to tension or compression [2]. The study of auxetic structures is receiving increasing attention, and researchers have explored various two-dimensional and three-dimensional structures [3]. In this research, we focus on the internal honeycomb structure. Gibson et al.[4] introduced the internal honeycomb structure in 1982. When this structure experiences tension, the diagonal sides of the cells move outward in the vertical direction, causing the structure to expand in the transverse direction [5]. In reviewing previous studies, Pakrooyan et al. [6] analyzed the parameters of a sandwich sheet with an auxetic core embedded in an ideal fluid matrix. They investigated the free vibration of sandwich panels using the second-order Frostig model for the auxetic core with a honeycomb structure and the first-order shear deformation theory (FSDT) for the cover sheets. In another study, Khorshidi et al. [7] explored energy harvesting in a sandwich sheet with an auxetic core featuring a honeycomb structure. Their investigation considered procedures reinforced with carbon nanolayers. Shabani and colleagues have investigated the buckling in porous beams made of graded functional materials [8]. Buckling, defined as the point of instability in the static behavior of cylinders subjected to external loads, plays a crucial role in these studies [9]. In 1941, Von Kármán and Tessin conducted initial studies on the static stability of thin-walled cylindrical shells

under axial load. They developed and presented a nonlinear theory to explain the significant discrepancies between experimental results and linear theories [10]. The proposed nonlinear theory introduced a form of radial deformation capable of reproducing the diamond-shaped pattern observed in experimental buckling tests. In a subsequent book written in 1983, Babcock examined many related articles [11]. In this book, static buckling, dynamic buckling, post-buckling, plastic, and elastic buckling with and without consideration of imperfections have been investigated. He also investigated the sensitivity of each defect by conducting various experimental tests. It has now been shown that geometric defects are the most influential and essential defects, and converting them into known factors is not easy. In 1984, Yamaki [12] conducted an extensive investigation into the impact of geometrical defects on the buckling behavior of thin-walled cylindrical shells. His study encompassed theoretical, numerical, and experimental approaches. Subsequently, in 1995, Kaladin [13] emphasized the significance of initial stresses resulting from geometrical imperfections and unspecified boundary conditions in influencing shell buckling performance. Kaladin also introduced intriguing relationships for approximating buckling predictions. He investigated simultaneous buckling modes and concluded that it is crucial to consider geometrical defects and locked stresses when analyzing buckling. These defects can arise from boundary conditions. In 2001, Elishakoff et al. [14] studied buckling behavior in shells with variable thickness. Additionally, Gonçalves and Del Prado investigated dynamic buckling in a flawless cylindrical shell subjected to static and dynamic axial loading 2002 [15]. In 2015, Thomson and Micheal conducted theoretical and experimental investigations on shell buckling using an energy-based approach. Their study also explored shock sensitivity in incompressible thin shells [16]. In 2018, Kumar and Srinivasa published a review article on buckling and free vibration of composite cylindrical sheets and shells [17]. Evkin et al. (2019) also studied local buckling in isotropic cylinders. Various cylindrical shell configurations were analyzed under different disturbance conditions [18]. In 2019, Ly et al. investigated the nonlinear buckling behaviour of a carbon nanotube-reinforced cylindrical shell. They examined the impact of auxetic core, carbon distribution, and volume fraction on the critical buckling load [19]. In 2020, Guo et al. employed finite element methods to explore the behaviour of cylindrical shells composed of various auxetic structures. Additionally, their study analyzed energy absorption in these different structures [20].

In this study, the effect of the presence of an auxetic structure (2D Re-entrant honeycomb) as the central layer in a three-layer cylindrical shell is investigated. Donell's theory is widely used in other papers. In this study, the modified shear deformation theory is used, and four kinds of functions, exponential, trigonometric, hyperbolic, and parabolic, are applied, and the results are compared. Aluminum is considered the material for all three layers, including the inner and outer layers of the isotropic shell. Additionally, the axial and static load is modeled as the pressure applied to the surface of the shell. In this study, modified shear deformation theory and Golerkin's numerical solution method were used, and the effect of the presence of an austic core on the buckling behavior of a three-layered cylindrical shell was investigated. The finite element software validated the results of the equations and used them for a layered cylindrical shell. Finally, the impact of parameters such as length-to-radius ratio, core thickness-to-total thickness ratio, and cell angle of the auxetic structure is investigated, and the results are presented. It was seen that increasing the length-to-radius ratio in a relatively thick shell (h/R =0.1) reduces the stiffness required for buckling by 25%. In the thinner shell (h/R =0.05), the system's stability decreases with the increase of the length-to-radius ratio, and for the value of 10, it almost disappears. With the most minor force, the system buckles experimentally. By examining the effect of the ratio of the thickness of the auxetic layer to the thickness of the shell, it was seen that for a thin shell (h/R =0.01), the system's stability is shallow, and the change of the said ratio does not have a significant effect. However, increasing the auxetic layer's thickness for relatively thicker shells reduces the system's stability more strongly. It was also seen that changing the angle in the auxetic cell does not significantly change the system's stability.

2- Define the problem:

A three-layered cylindrical shell with length L, radius R, and total thickness h is considered as in Fig.1. To facilitate the mathematical modeling of the problem, a cylindrical coordinate system with x, θ, and z components has been used. The purpose of this research is to investigate the buckling behavior of the mentioned cylindrical shell.

3- Formulation of a three-layer cylindrical shell with an auxetic core:

To investigate the buckling behavior, it is assumed that the cylindrical shell is subjected to a uniform axial load, and Eq.(1) has been used [21]:

$$\int_0^t (\delta U_{shell} + \delta V)dt = 0 \tag{1}$$

where δU_{shell} is the potential energy changes of the shell, and δV is the potential energy changes caused by the axial load N_0. By using the theory of modified shear deformation of Eqs. (2), the governing equations of the system can be reached [17].

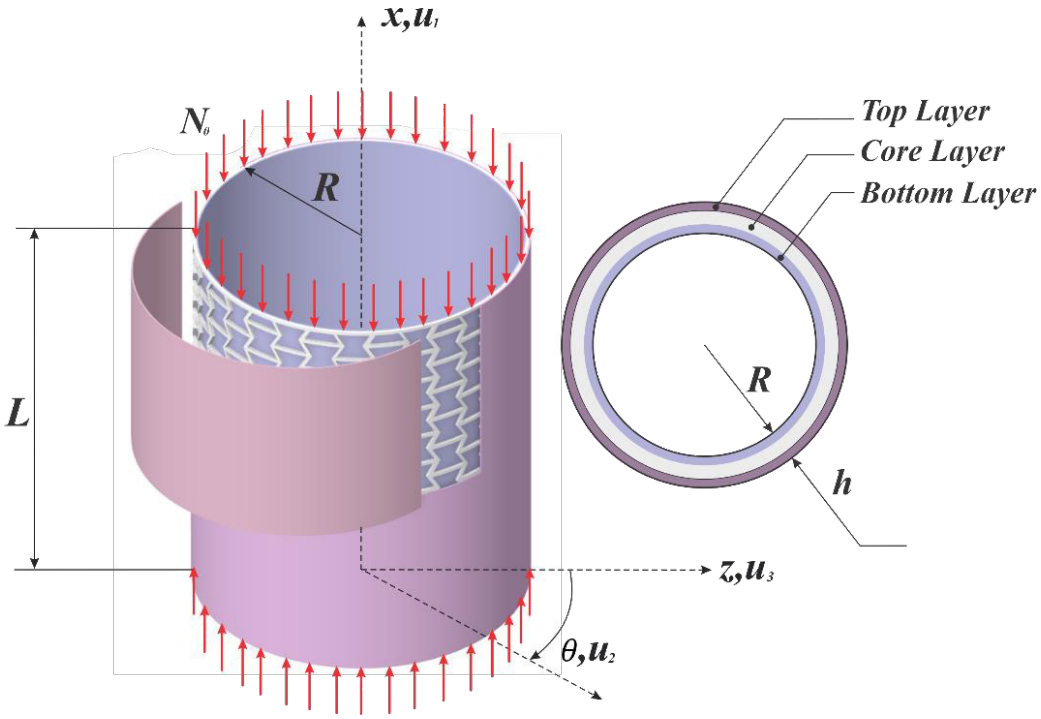

Fig. 1. Definition of cylindrical coordinates for a three-layer shell under axial loading

$$u_1(x,\theta,z,t)=u(x,\theta,t)-f_1(z)\frac{\partial w(x,\theta,t)}{\partial x}+f_2(z)\varphi_1(x,\theta,t) \quad \text{(a)}$$

$$u_2(x,\theta,z,t)=v(x,\theta,t)-\frac{f_1(z)}{R}\left(\frac{\partial w(x,\theta,t)}{\partial \theta}-v(x,\theta,t)\right)+f_2(z)\varphi_2(x,\theta,t) \quad \text{(b)} \quad (2)$$

$$u_3(x,\theta,z,t)=w(x,\theta,t) \quad \text{(c)}$$

where $u(x,\theta,t), v(x,\theta,t), w(x,\theta,t)$ represent longitudinal, circumferential and transverse, respectively displacement of the cylindrical shell and $\varphi_1(x,\theta,t), \varphi_2(x,\theta,t)$ represent the rotation of the middle plane around the x and θ axes, respectively. $f_1(z), f_2(z)$ are also considered based on different theories as in Table 1.

Assuming linearity, the strain-displacement relations for a cylindrical shell will be in the form of Eqs. (3) [4, 5]:

$$\varepsilon_{xx}=\frac{\partial u_1}{\partial x}=\frac{\partial u_0}{\partial x}+f_1(z)\frac{\partial^2 w_0}{\partial x^2}+f_2(z)\frac{\partial \phi_1}{\partial x} \quad \text{(a)}$$

$$\varepsilon_{\theta\theta}=\frac{1}{R}\left(\frac{\partial u_2}{\partial x}+u_3\right)=\frac{1}{R}\left(w_0+\frac{\partial v_0}{\partial \theta}\right)+\frac{f_1(z)}{R^2}\left(\frac{\partial^2 w_0}{\partial \theta^2}-\frac{\partial v_0}{\partial \theta}\right)+\frac{f_2(z)}{R}\frac{\partial \phi_2}{\partial \theta} \quad \text{(b)} \quad (3)$$

$$\gamma_{x\theta}=\frac{1}{R}\frac{\partial u_1}{\partial \theta}+\frac{\partial u_2}{\partial x}=\frac{\partial v_0}{\partial x}+\frac{f_1(z)}{R}\left(\frac{\partial^2 w_0}{\partial x\,\partial \theta}-\frac{\partial v_0}{\partial x}\right)+\frac{1}{R}\left(\frac{\partial u_0}{\partial \theta}+f_1(z)\frac{\partial^2 w_0}{\partial x\,\partial \theta}+f_2(z)\frac{\partial \phi_1}{\partial \theta}\right)+f_2(z)\frac{\partial \phi_2}{\partial x} \quad \text{(c)}$$

Table 1. Mathematical theories for modeling configurations [22]

	Theory	$f_1(z)$	$f_2(z)$
ESDPT	Exponential	$-z$	$ze^{-2\left(\frac{z}{h}\right)^2}$
TSDPT	Trigonometric	$-z$	$\frac{h}{\pi}\sin\left(\frac{\pi z}{h}\right)$
HSDPT	Hyperbolic	$-z$	$h\sinh\left(\frac{z}{h}\right)-z\cosh\left(\frac{1}{2}\right)$
PSDPT	Parabolic	$-z$	$z\left(\frac{5}{4}-\frac{5}{3h^2}z^2\right)$

$$\gamma_{xz}=\frac{\partial u_3}{\partial x}+\frac{\partial u_1}{\partial z}=\frac{\partial w_0}{\partial x}\left(1+\frac{\partial f_1(z)}{\partial z}\right)+\frac{\partial f_2(z)}{\partial z}\phi_1 \quad \text{(d)}$$

$$\gamma_{\theta z}=\frac{1}{R}\frac{\partial u_3}{\partial \theta}+\frac{\partial u_2}{\partial z}-\frac{u_2}{R}= \quad (3)$$

$$\left(1+\frac{\partial f_1(z)}{\partial z}\right)\left(\frac{1}{R}\frac{\partial w_0}{\partial \theta}-\frac{v_0}{R}\right)+\frac{\partial f_2(z)}{\partial z}\phi_2 \quad \text{(e)}$$

Also, the structural relations of the three-layer cylindrical shell are defined as Eq. (4) [6]:

$$\begin{Bmatrix}\sigma_{xx}\\ \sigma_{\theta\theta}\\ \sigma_{\theta z}\\ \sigma_{xz}\\ \sigma_{x\theta}\end{Bmatrix}^{(k)}=\begin{bmatrix}Q_{11}^{(k)} & Q_{12}^{(k)} & 0 & 0 & 0\\ Q_{21}^{(k)} & Q_{22}^{(k)} & 0 & 0 & 0\\ 0 & 0 & Q_{44}^{(k)} & 0 & 0\\ 0 & 0 & 0 & Q_{55}^{(k)} & 0\\ 0 & 0 & 0 & 0 & Q_{66}^{(k)}\end{bmatrix}\cdot\begin{Bmatrix}\varepsilon_{xx}\\ \varepsilon_{\theta\theta}\\ \gamma_{\theta z}\\ \gamma_{xz}\\ \gamma_{x\theta}\end{Bmatrix} \quad (4)$$

where the superscript k represents the layer number. The dimensions of the stiffness matrix for layers first and third are defined as Eqs. (5). These two layers are made of aluminum and are assumed to be isotropic[6].

$$Q_{11}^{(1,3)}=Q_{22}^{(1,3)}=\frac{E}{1-\nu^2} \quad \text{(a)}$$

$$Q_{12}^{(1,3)}=Q_{21}^{(1,3)}=\frac{\nu E}{1-\nu^2} \quad \text{(b)} \quad (5)$$

$$Q_{44}^{(1,3)}=Q_{55}^{(1,3)}=Q_{66}^{(1,3)}=G=\frac{E}{2(1+\nu)} \quad \text{(c)}$$

where E, G and ν are Young's modulus, shear modulus, and Poisson's ratio of aluminum, respectively. The properties of the auxetic layer ($k=2$), according to the assumed structure, which in this research is considered as a re-internal honeycomb structure according to Fig.2, are obtained from Eqs. (6) [6].

$$E_1^{(2)}=E_s\frac{\left(\eta_3\sec\theta_1\right)^3(\eta_1+\sin\theta_1)}{\left[1+\eta_3^2\left(\tan^2\theta_1+\eta_1\eta_2 sec^2\theta_1\right)\right]} \quad \text{(a)}$$

$$E_2^{(2)}=E_s\frac{{\eta_3}^3\sec\theta_1}{(\eta_1+\sin\theta_1)\left(\tan^2\theta_1+\eta_3^2\right)} \quad \text{(b)}$$

$$G_{12}^{(2)}=E_s\frac{\eta_3^3\sec\theta_1(\eta_1+\sin\theta_1)}{\eta_1^2\left(1+2\eta_1\eta_2^3\right)} \quad \text{(c)}$$

$$G_{23}^{(2)}=G_s\frac{\eta_3\cos\theta_1}{\eta_1+\sin\theta_1} \quad \text{(d)} \quad (6)$$

$$G_{31}^{(2)}=G_s\frac{\eta_3\sec\theta_1}{2\eta_2(\eta_1+\sin\theta_1)(\eta_1+2\eta_2)} \quad \text{(e)}$$

$$\nu_{12}^{(2)}=\frac{\sec\theta_1\tan\theta_1\left(1-{\eta_3}^2\right)(\eta_1+\sin\theta_1)}{\left[1+\left(\tan^2\theta_1+\eta_1\eta_2 sec^2\theta_1\right)\eta_3^2\right]} \quad \text{(f)}$$

$$\nu_{21}^{(2)}=\frac{\sin\theta_1\left(1-\eta_3^2\right)}{\left(\tan^2\theta_1+\eta_3^2\right)(\eta_1+\sin\theta_1)} \quad \text{(g)}$$

$$\rho^{(2)}=\rho_s\frac{\eta_3(\eta_1+2)}{2cos\theta_1\ (\eta_1+\sin\theta_1)} \quad \text{(h)}$$

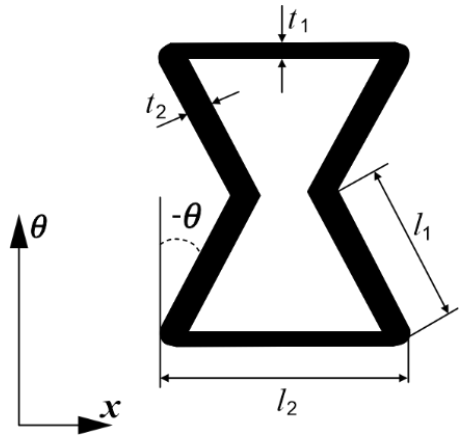

Fig. 2. A Re-internal Honeycomb Cell Structure [20]

where $\eta_1=\frac{l_2}{l_1}$, $\eta_2=\frac{t_2}{t_1}$, $\eta_3=\frac{t_1}{l_1}$, G_s and E_s are the elastic properties and ρ_s is the density of the material that makes up the auxetic core, which here is made of aluminum. Eq.(7) is used to obtain changes in shell strain energy[7].

$$U=\frac{1}{2}\sum_{k=1}^{3}\int_{\forall^{(k)}}\left(\left\{\sigma_{xx},\sigma_{\theta\theta},\sigma_{x\theta},\sigma_{xz},\sigma_{\theta z}\right\}^{(k)}\cdot\left\{\varepsilon_{xx},\varepsilon_{\theta\theta},\gamma_{x\theta},\gamma_{xz},\gamma_{\theta z}\right\}\right)d\forall^{(k)} \tag{7}$$

By placing the strain-displacement equations and then partially integrating, the strain energy changes for the cylindrical shell can be obtained in the form of Eq.(8) [23]:

$$\delta U=\int_A\begin{pmatrix}-\frac{\partial N_{xx}}{\partial x}\delta u_0+\frac{\partial^2 S_{xx}}{\partial x^2}\delta w_0-\frac{\partial P_{xx}}{\partial x}\delta\phi_1\\-\frac{1}{R}\frac{\partial N_{\theta\theta}}{\partial\theta}\delta v_0+\frac{1}{R^2}\frac{\partial^2 S_{\theta\theta}}{\partial\theta^2}\delta w_0\\+\frac{1}{R^2}\frac{\partial S_{\theta\theta}}{\partial\theta}\delta v_0-\frac{1}{R}\frac{\partial P_{\theta\theta}}{\partial\theta}\delta\phi_2\\+\frac{N_{\theta\theta}}{R}\delta w_0-\frac{\partial N_{x\theta}}{\partial x}\delta v_0+\frac{2}{R}\frac{\partial^2 S_{x\theta}}{\partial x\,\partial\theta}\delta w_0\\+\frac{1}{R}\frac{\partial S_{x\theta}}{\partial x}\delta v_0-\frac{\partial P_{x\theta}}{\partial x}\delta\phi_2-\frac{1}{R}\frac{\partial N_{x\theta}}{\partial x}\delta u_0\\-\frac{1}{R}\frac{\partial P_{x\theta}}{\partial\theta}\delta\phi_1-\frac{\partial T_{xz}}{\partial x}\delta w_0+Q_{xx}\delta\phi_1\\-\frac{1}{R}\frac{\partial T_{\theta z}}{\partial\theta}\delta w_0-\frac{T_{\theta z}}{R}\delta v_0+Q_{\theta z}\delta\phi_2\end{pmatrix}dA \tag{8}$$

that the forces and moments are defined in the form of Eqs. (9) [23]:

$$\left\{N_{xx},N_{\theta\theta},N_{x\theta}\right\}=\sum_{k=1}^{3}\int_{z_{k-1}}^{z_k}\left\{\sigma_{xx},\sigma_{\theta\theta},\sigma_{x\theta}\right\}^{(k)}dz \tag{a}$$

$$\left\{S_{xx},S_{\theta\theta},S_{x\theta}\right\}=\sum_{k=1}^{3}\int_{z_{k-1}}^{z_k}\left\{\sigma_{xx},\sigma_{\theta\theta},\sigma_{x\theta}\right\}^{(k)}f_1(z)dz \tag{b}$$

$$\left\{P_{xx},P_{\theta\theta},P_{x\theta}\right\}=\sum_{k=1}^{3}\int_{z_{k-1}}^{z_k}\left\{\sigma_{xx},\sigma_{\theta\theta},\sigma_{x\theta}\right\}^{(k)}f_2(z)dz \tag{c}$$

$$\left\{Q_{xz},Q_{\theta z}\right\}=\sum_{k=1}^{3}\int_{z_{k-1}}^{z_k}\left\{\sigma_{xz},\sigma_{\theta z}\right\}^{(k)}\frac{\partial f_2(z)}{\partial z}dz \tag{d}$$

$$\left\{T_{xz},T_{\theta z}\right\}=\sum_{k=1}^{3}\int_{z_{k-1}}^{z_k}\left\{\sigma_{xz},\sigma_{\theta z}\right\}^{(k)}\left(\frac{\partial f_1(z)}{\partial z}+1\right)dz \tag{e}$$

(9)

Also, potential energy changes due to axial loading will be N_0 and is obtained by Eq.(10) [7]:

$$\delta V=\int_0^L\int_0^{2\pi}-\left(N_0\frac{\partial^2 w_0}{\partial x^2}\delta w_0+N_0\frac{\partial^2 v_0}{\partial x^2}\delta v_0\right)Rd\theta dx \tag{10}$$

By substituting Eq.(8) and Eq.(10) in Eq.(1), the governing equations of the system are obtained in the form of Eqs. (11) [24].

$$\delta u_0: \quad \frac{\partial N_{xx}}{\partial x}+\frac{1}{R}\frac{\partial N_{x\theta}}{\partial \theta}=0 \qquad \text{(a)}$$

$$\delta v_0: \frac{1}{R}\frac{\partial N_{\theta\theta}}{\partial \theta}-\frac{1}{R^2}\frac{\partial S_{\theta\theta}}{\partial \theta}+\frac{\partial N_{x\theta}}{\partial x} -\frac{1}{R}\frac{\partial S_{x\theta}}{\partial x}+\frac{T_{\theta z}}{R}+N_0\frac{\partial^2 v_0}{\partial x^2}=0 \qquad \text{(b)}$$

$$\delta w_0: \frac{\partial T_{xz}}{\partial x}+\frac{1}{R}\frac{\partial T_{\theta z}}{\partial \theta}-\frac{\partial^2 S_{xx}}{\partial x^2} -\frac{1}{R^2}\frac{\partial^2 S_{\theta\theta}}{\partial \theta^2}-\frac{N_{\theta\theta}}{R}-\frac{2}{R}\frac{\partial^2 S_{x\theta}}{\partial x\,\partial \theta} +N_0\frac{\partial^2 w_0}{\partial x^2}=0 \qquad \text{(c)} \qquad (11)$$

$$\delta \phi_1: \frac{\partial P_{xx}}{\partial x}+\frac{1}{R}\frac{\partial P_{x\theta}}{\partial \theta}-Q_{xz}=0 \qquad \text{(d)}$$

$$\delta \phi_2: \frac{\partial P_{x\theta}}{\partial x}+\frac{1}{R}\frac{\partial P_{\theta\theta}}{\partial \theta}-Q_{\theta z}=0 \qquad \text{(e)}$$

The equations of Eqs. (11) are in terms of force and moment, and they can be written in terms of displacement as Eq.(12) to Eq.(16):

$$\begin{aligned}\delta u_0 =& \frac{A_1}{R}\left(\frac{\partial^2 v_0}{\partial \theta \partial \theta}+\frac{\partial w_0}{\partial x}\right)+\frac{A_2}{R}\frac{\partial^2 \phi_2}{\partial x\,\partial \theta} +\frac{A_4}{R^2}\left(\frac{\partial^3 w_0}{\partial x\,\partial \theta^2}-\frac{\partial^2 v_0}{\partial x\,\partial \theta}\right)+B_1\frac{\partial^2 u_0}{\partial x^2} +B_2\frac{\partial^2 \phi_1}{\partial x^2}+B_3\frac{\partial^3 w_0}{\partial x^3}+\frac{1}{R}(C_1\frac{\partial^2 v_0}{\partial x\,\partial \theta} +C_2\frac{\partial^2 \phi_2}{\partial x\,\partial \theta}+\frac{C_3}{R}\left(2\frac{\partial^3 w_0}{\partial x\,\partial \theta^2}-\frac{\partial^2 v_0}{\partial x\,\partial \theta}\right) +\frac{C_1}{R}\frac{\partial^2 u_0}{\partial \theta^2}+\frac{C_2}{R}\frac{\partial^2 \phi_1}{\partial \theta^2})=0\end{aligned} \qquad (12)$$

$$\begin{aligned}\delta v_0: & \frac{1}{R}(\frac{F_1}{R}\left(\frac{\partial^2 v_0}{\partial \theta^2}+\frac{\partial w_0}{\partial \theta}\right)+\frac{F_2}{R}\frac{\partial^2 \phi_2}{\partial \theta^2} +\frac{F_3}{R^2}\left(\frac{\partial^3 w_0}{\partial \theta^3}-\frac{\partial^2 v_0}{\partial \theta^2}\right)+A_1\frac{\partial^2 u_0}{\partial x\,\partial \theta} +A_2\frac{\partial^2 \phi_1}{\partial x\,\partial \theta}+A_3\frac{\partial^3 w_0}{\partial x^2\partial \theta})-\frac{1}{R^2}(\frac{F_3}{R}\left(\frac{\partial^2 v_0}{\partial \theta^2}+\frac{\partial w_0}{\partial \theta}\right) +\frac{F_4}{R}\frac{\partial^2 \phi_2}{\partial \theta^2}+\frac{F_5}{R^2}\left(\frac{\partial^3 w_0}{\partial \theta^3}-\frac{\partial^2 v_0}{\partial \theta^2}\right)+A_3\frac{\partial^2 u_0}{\partial x\,\partial \theta} +A_4\frac{\partial^2 \phi_1}{\partial x\,\partial \theta}+A_5\frac{\partial^3 w_0}{\partial x^2\partial \theta})+C_1\frac{\partial^2 v_0}{\partial x^2}+C_2\frac{\partial^2 \phi_2}{\partial x^2} +\frac{C_3}{R}\left(2\frac{\partial^3 w_0}{\partial x^2\partial \theta}-\frac{\partial^2 v_0}{\partial x^2}\right)+\frac{C_1}{R}\frac{\partial^2 u_0}{\partial x\,\partial \theta}+\frac{C_2}{R}\frac{\partial^2 \phi_1}{\partial x\,\partial \theta} -\frac{1}{R}(C_3\frac{\partial^2 v_0}{\partial x^2}+C_4\frac{\partial^2 \phi_2}{\partial x^2}+\frac{C_5}{R}\left(2\frac{\partial^3 w_0}{\partial x^2\partial \theta}-\frac{\partial^2 v_0}{\partial x^2}\right) +\frac{C_3}{R}\frac{\partial^2 u_0}{\partial x\,\partial \theta}+\frac{C_4}{R}\frac{\partial^2 \phi_1}{\partial x\,\partial \theta})+\frac{1}{R}((D_3+D_4)\phi_2 +\frac{(D_1+2D_2+D_5)}{R}\left(\frac{\partial w_0}{\partial \theta}-v_0\right))+N_0\frac{\partial^2 v_0}{\partial x^2}=0\end{aligned} \qquad (13)$$

$$\begin{aligned}\delta w_0: & (E_3+E_4)\frac{\partial \phi_1}{\partial x}+(E_1+2E_2+E_5)\frac{\partial^2 w_0}{\partial x^2} +\frac{1}{R}((D_3+D_4)\frac{\partial \phi_2}{\partial \theta} +\frac{(D_1+2D_2+D_5)}{R}\left(\frac{\partial^2 w_0}{\partial \theta^2}-\frac{\partial v_0}{\partial \theta}\right)) -\frac{A_3}{R}\left(\frac{\partial^3 v_0}{\partial x^2\partial \theta}+\frac{\partial^2 w_0}{\partial x^2}\right)-\frac{A_4}{R}\frac{\partial^3 \phi_2}{\partial x^2\partial \theta} -\frac{A_5}{R^2}\left(\frac{\partial^4 w_0}{\partial x^2\partial \theta^2}-\frac{\partial^3 v_0}{\partial x^2\partial \theta}\right)-B_3\frac{\partial^3 u_0}{\partial x^3} -B_4\frac{\partial^3 \phi_1}{\partial x^3}-B_5\frac{\partial^4 w_0}{\partial x^4}-\frac{1}{R^2}(\frac{F_3}{R}\left(\frac{\partial^3 v_0}{\partial \theta^3}+\frac{\partial^2 w_0}{\partial \theta^2}\right) +\frac{F_4}{R}\frac{\partial^3 \phi_2}{\partial \theta^3}+\frac{F_5}{R^2}\left(\frac{\partial^4 w_0}{\partial \theta^4}-\frac{\partial^3 v_0}{\partial \theta^3}\right)+A_3\frac{\partial u_0}{\partial x} +A_4\frac{\partial^3 \phi_1}{\partial x\,\partial \theta^2}+A_5\frac{\partial^4 w_0}{\partial x^2\partial \theta^2})-\frac{1}{R}(\frac{F_1}{R}\left(\frac{\partial v_0}{\partial \theta}+w_0\right) +\frac{F_2}{R}\frac{\partial \phi_2}{\partial \theta}+\frac{F_3}{R^2}\left(\frac{\partial^2 w_0}{\partial \theta^2}-\frac{\partial v_0}{\partial \theta}\right)+A_1\frac{\partial u_0}{\partial x} +A_2\frac{\partial \phi_1}{\partial x}+A_3\frac{\partial^2 w_0}{\partial x^2})-\frac{2}{R}(C_3\frac{\partial^3 v_0}{\partial x^2\partial \theta} +C_4\frac{\partial^3 \phi_2}{\partial x^2\partial \theta}+\frac{C_5}{R}\left(2\frac{\partial^4 w_0}{\partial x^2\partial \theta^2}-\frac{\partial^3 v_0}{\partial x^2\partial \theta}\right) +\frac{C_3}{R}\frac{\partial^3 u_0}{\partial x\,\partial \theta^2}+\frac{C_4}{R}\frac{\partial^3 \phi_1}{\partial x\,\partial \theta^2})+N_0\frac{\partial^2 w_0}{\partial x^2}=0\end{aligned} \qquad (14)$$

$$\delta\phi_1 : \frac{A_2}{R}\left(\frac{\partial^2 v_0}{\partial x\,\partial\theta}+\frac{\partial w_0}{\partial x}\right)+\frac{A_6}{R}\frac{\partial^2\phi_2}{\partial x\,\partial\theta}$$
$$+\frac{A_4}{R^2}\left(\frac{\partial^3 w_0}{\partial x\,\partial\theta^2}-\frac{\partial^2 v_0}{\partial x\,\partial\theta}\right)+B_2\frac{\partial^2 u_0}{\partial x^2}$$
$$+B_6\frac{\partial^2\phi_1}{\partial x^2}+B_4\frac{\partial^3 w_0}{\partial x^3}+\frac{1}{R}(C_2\frac{\partial^2 v_0}{\partial x\,\partial\theta}$$
$$+C_6\frac{\partial^2\phi_2}{\partial x\,\partial\theta}+\frac{C_4}{R}\left(2\frac{\partial^3 w_0}{\partial x\,\partial\theta^2}-\frac{\partial^2 v_0}{\partial x\,\partial\theta}\right)$$
$$+\frac{C_2}{R}\frac{\partial^2 u_0}{\partial\theta^2}+\frac{C_6}{R}\frac{\partial^2\phi_1}{\partial\theta^2})$$
$$-E_6\phi_1-(E_3+E_4)\frac{\partial w_0}{\partial x}=0 \qquad (15)$$

$$\delta\phi_2 : C_2\frac{\partial^2 v_0}{\partial x^2}+C_6\frac{\partial^2\phi_2}{\partial x^2}$$
$$+\frac{C_4}{R}\left(2\frac{\partial^3 w_0}{\partial x^2\partial\theta}-\frac{\partial^2 v_0}{\partial x^2}\right)+\frac{C_2}{R}\frac{\partial^2 u_0}{\partial x\,\partial\theta}$$
$$+\frac{C_6}{R}\frac{\partial^2\phi_1}{\partial x\,\partial\theta}+\frac{1}{R}(\frac{F_2}{R}\left(\frac{\partial^2 v_0}{\partial\theta^2}+\frac{\partial w_0}{\partial\theta}\right)$$
$$+\frac{F_6}{R}\frac{\partial^2\phi_2}{\partial\theta^2}+\frac{F_4}{R^2}\left(\frac{\partial^3 w_0}{\partial\theta^3}-\frac{\partial^2 v_0}{\partial\theta^2}\right)$$
$$+A_2\frac{\partial^2 u_0}{\partial x\,\partial\theta}+A_6\frac{\partial^2\phi_1}{\partial x\,\partial\theta}+A_4\frac{\partial^3 w_0}{\partial x^2\partial\theta})$$
$$-\frac{(D_3+D_4)}{R}\left(\frac{\partial w_0}{\partial\theta}-v_0\right)-D_6\phi_2=0 \qquad (16)$$

where A_i, B_i, C_i, D_i, E_i and F_i are:

$$\{A_1,A_2,A_3,A_4,A_5,A_6\}=$$
$$\sum_{k=1}^{3}\int_{z_{k-1}}^{z_k} Q_{12}^{(k)}\{1,f_2,f_1,f_1f_2,f_1^2,f_2^2\}\,dz \qquad (a)$$

$$\{B_1,B_2,B_3,B_4,B_5,B_6\}=$$
$$\sum_{k=1}^{3}\int_{z_{k-1}}^{z_k} Q_{11}^{(k)}\{1,f_2,f_1,f_1f_2,f_1^2,f_2^2\}\,dz \qquad (b)$$

$$\{C_1,C_2,C_3,C_4,C_5,C_6\}=$$
$$\sum_{k=1}^{3}\int_{z_{k-1}}^{z_k} Q_{66}^{(k)}\{1,f_2,f_1,f_1f_2,f_1^2,f_2^2\}\,dz \qquad (c) \qquad (17)$$

$$\{D_1,D_2,D_3,D_4,D_5,D_6\}=$$
$$\sum_{k=1}^{3}\int_{z_{k-1}}^{z_k} Q_{44}^{(k)}\{1,\frac{\partial f_1}{\partial z},\frac{\partial f_2}{\partial z},\frac{\partial f_1}{\partial z}\frac{\partial f_2}{\partial z}$$
$$,\left(\frac{\partial f_1}{\partial z}\right)^2,\left(\frac{\partial f_2}{\partial z}\right)^2\}\,dz \qquad (d)$$

$$\{E_1,E_2,E_3,E_4,E_5,E_6\}=$$
$$\sum_{k=1}^{3}\int_{z_{k-1}}^{z_k} Q_{55}^{(k)}\{1,\frac{\partial f_1}{\partial z},\frac{\partial f_2}{\partial z},\frac{\partial f_1}{\partial z}\frac{\partial f_2}{\partial z}$$
$$,\left(\frac{\partial f_1}{\partial z}\right)^2,\left(\frac{\partial f_2}{\partial z}\right)^2\}dz \qquad (e) \qquad (17)$$

$$\{F_1,F_2,F_3,F_4,F_5,F_6\}=$$
$$\sum_{k=1}^{3}\int_{z_{k-1}}^{z_k} Q_{22}^{(k)}\{1,f_2,f_1,f_1f_2,f_1^2,f_2^2\}dz \qquad (f)$$

4- Solving the governing equations of the system:

In this study, the simply supported boundary conditions are chosen in the following circumestances[25]:

$$v=w=0,\frac{\partial^2 v}{\partial x^2}=\frac{\partial^2 w}{\partial x^2}=0, x=0,L \qquad (18)$$

The numerical Galerkin method is considered to solve the governing equations of the system. The function of trying to solve the problem is assumed as Eqs.(19). Tried functions are not time-dependent because the problem is defined and solved statically [9].

$$u_0(x,\theta)=\sum_{\tilde{m}=1}^{\tilde{M}}\sum_{\tilde{n}=1}^{\tilde{N}}u_{\tilde{m}\tilde{n}}\overset{=}{u}_0(x,\theta) \qquad (a)$$
$$v_0(x,\theta)=\sum_{\tilde{m}=1}^{\tilde{M}}\sum_{\tilde{n}=1}^{\tilde{N}}v_{\tilde{m}\tilde{n}}\overset{=}{v}_0(x,\theta) \qquad (b)$$
$$w_0(x,\theta)=\sum_{\tilde{m}=1}^{\tilde{M}}\sum_{\tilde{n}=1}^{\tilde{N}}w_{\tilde{m}\tilde{n}}\overset{=}{w}_0(x,\theta) \qquad (c) \qquad (19)$$
$$\phi_1(x,\theta)=\sum_{\tilde{m}=1}^{\tilde{M}}\sum_{\tilde{n}=1}^{\tilde{N}}\phi_{1\tilde{m}\tilde{n}}\overset{=}{\phi}_1(x,\theta) \qquad (d)$$
$$\phi_2(x,\theta)=\sum_{\tilde{m}=1}^{\tilde{M}}\sum_{\tilde{n}=1}^{\tilde{N}}\phi_{2\tilde{m}\tilde{n}}\overset{=}{\phi}_2(x,\theta) \qquad (e)$$

Table 2. Critical load values of isotropic cylindrical shell buckling using mathematical equations and FEM

$R=1$ (m), $L=3$ (m) , $h=3$ (mm) , $E=70$ (GPa) , $\nu=0.3$

FEM	Exponential theory (present work)	Hyperbolic theory (present work)	Trigonometric theory (present work)	Parabolic theory (present work)
3.6281×10^5 (N)	3.64388×10^5 (N)	3.64388×10^5 (N)	3.64388×10^5 (N)	3.64388×10^5 (N)

In Eqs. (19) $u_{\tilde{m}\tilde{n}}, v_{\tilde{m}\tilde{n}}, w_{\tilde{m}\tilde{n}}, \phi_{1\tilde{m}\tilde{n}}$ and $\phi_{2\tilde{m}\tilde{n}}$ are unknown coefficients that are obtained after minimizing the error. $\overline{\overline{u}}_0(x,\theta), \overline{\overline{v}}_0(x,\theta), \overline{\overline{w}}_0(x,\theta), \overline{\overline{\phi}}_1(x,\theta)$ and $\overline{\overline{\phi}}_2(x,\theta)$ are tried functions that satisfy the boundary conditions and are considered the same weight functions in the Galerkin method. Tried functions for simply support conditions are considered as Eq.(20) [9].

$$\begin{cases} \overline{\overline{u}}_0(x,\theta)=\cos(\alpha_{\tilde{m}}x)\cos(\tilde{n}\theta) \\ \overline{\overline{v}}_0(x,\theta)=\sin(\alpha_{\tilde{m}}x)\sin(\tilde{n}\theta) \\ \overline{\overline{w}}_0(x,\theta)=\sin(\alpha_{\tilde{m}}x)cos(\tilde{n}\theta) \\ \overline{\overline{\phi}}_1(x,\theta)=\cos(\alpha_{\tilde{m}}x)cos(\tilde{n}\theta) \\ \overline{\overline{\phi}}_2(x,\theta)=\sin(\alpha_{\tilde{m}}x)\sin(\tilde{n}\theta) \end{cases} \text{ for S-S} \quad (20)$$

By putting the approximation functions in the governing Eq.(12) to Eq.(16), the system of equations is in the form Eq.(21):

$$\left[\mathbf{C_{ij}}\right]\{u_{\tilde{m}\tilde{n}}\ \ v_{\tilde{m}\tilde{n}}\ \ w_{\tilde{m}\tilde{n}}\ \ \phi_{1\tilde{m}\tilde{n}}\ \ \phi_{2\tilde{m}\tilde{n}}\}^T=0 \quad (i,j=1,\ldots,5) \quad (21)$$

By setting the determinant of the matrix of coefficients C_{ij} equal to zero, the critical load equation of the system can be obtained, which will be according to Eq.(22):

$$\gamma_1 N_{cr}^2+\gamma_2 N_{cr}+\gamma_3=0 \quad (22)$$

where N_{cr} is the critical buckling load and γ_i are constant coefficients. By solving Eq.(22), the critical load of the system will be obtained.

5- Validation of results

To validate the relationships obtained in the previous section, the value of the critical buckling load for an isotropic cylinder was obtained using the assumed theory and compared with the results obtained from ABAQUS software for the same cylinder and finally presented in Table 2 and Fig. 3

The information presented in Table 2 indicates that the mathematical relationships obtained in the second part have appropriate accuracy.

6- Investigating the effect of different parameters of the cylindrical shell on the amount of critical load:

• Effect of length-to-radius ratio on critical load:

The effect of the ratio of length to radius *(L/R)* on the critical load for thin and relatively thick shells with the boundary conditions of two simple support ends is presented in Table 3. It can be seen that in thin and relatively thick shells, the critical load decreases continuously with the increase in the ratio of the length to the radius of the shell. It should be noted that with the increase of the mentioned ratio, the stiffness of the structure and the stability of the system will decrease, and the shell will experience buckling with less load.

• The effect of the ratio of the thickness of the auxetic core to the total thickness (h_c/h) on the critical load:

The effect of the ratio of core thickness to total thickness (h_c/h) in thin and relatively thick shells with the boundary conditions of two simple support ends is shown in Table 4. A decreasing trend can be seen by increasing the ratio of the core thickness to the total thickness. Due to the existence of the internal honeycomb structure and the behavior characteristic of this structure against the compressive force, it is predictable to observe a downward trend for the critical load and a decrease in the stability of the system.

• The effect of the cell angle of the auxetic structure on the amount of critical load

The parameter θ is known as the cell angle in the auxetic

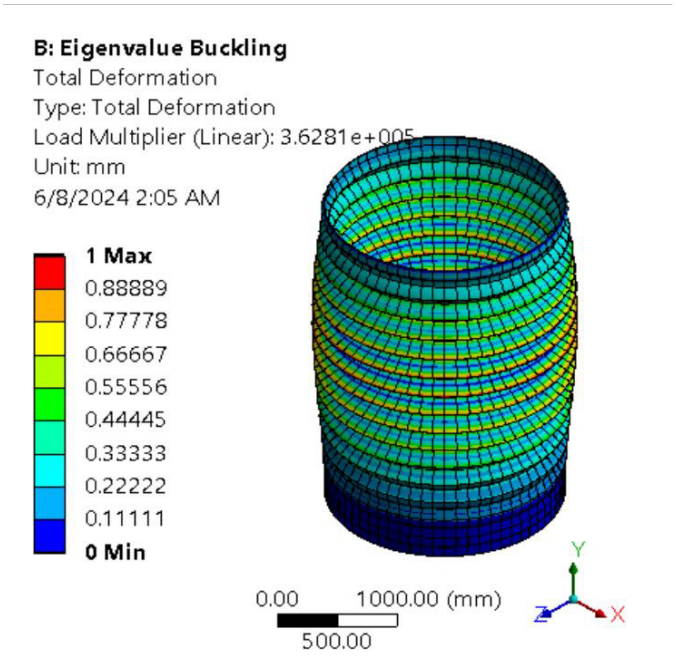

Fig. 3. Verifing Equations With FEM Analysis

Table 3. Critical buckling load of the cylindrical shell according to the change of the length-to-radius ratio and the thickness ratio of the cylindrical shell (× 10^6)

L/R	$h/R=0.01$	$h/R=0.05$	$h/R=0.08$
1	3.31232	76.9195	186.321
3	3.0178	73.7303	163.539
5	2.86879	67.6411	151.131
7	2.85157	55.6731	140.711
10	2.67397	54.5211	132.14

Table 4. The effect of the ratio of the thickness of the auxetic core on the total thickness of the critical buckling load (× 10^6)

h_c/h	$h/R=0.01$	$h/R=0.05$	$h/R=0.1$
0	3.4405	66.442	278.734
0.1	3.24009	62.2526	269.675
0.2	3.03105	57.9082	259.221
0.3	2.80475	53.2584	238.699
0.4	2.55259	48.1519	211.742
0.5	2.26593	42.4357	182.701
0.6	1.93612	35.9542	151.042
0.7	1.55452	28.5516	116.267
0.8	1.11265	20.1073	56.1987
0.9	0.603331	6.77047	14.9217

Table 5. The effect of the thickness-to-total thickness ratio of the auxetic core and cell angle on the critical load (× 10^6)

h_c / h	$\theta = -10$	$\theta = -30$	$\theta = -45$	$\theta = -60$	$\theta = -80$
0.1	3.239	3.23975	3.24009	3.24055	3.24368
0.2	3.02891	3.03037	3.03105	3.03195	3.03827
0.3	2.80163	2.830377	2.80475	2.80608	2.81546
0.4	2.5486	2.55135	2.55259	2.55432	2.56682
0.5	2.26122	2.26449	2.26593	2.26802	2.28363
0.6	1.93088	1.93457	1.93612	1.93854	1.95727
0.7	1.54895	1.55294	1.55452	1.55819	1.57887
0.8	1.10699	1.11114	1.11265	1.11542	1.13977
0.9	0.58856	0.60047	0.60333	0.60616	0.63222

structure. (Refer to Fig.2) The more significant the absolute value of this angle, the greater the rigidity and density of the system, and as a result, the system's stability is expected to be more significant. The data presented in Table 5 confirm this fact. Of course, this increase in stability happens with a minimal slope. On the other hand, according to the data in Table 5, it can be seen that the effect of the ratio of the core thickness to the total thickness on the system's stability is significant and more effective than the angle changes in the auxetic cell. The reason for this issue was also discussed in the previous section.

7- Conclusion and summary:

In this study, the mathematical relationships governing the buckling phenomenon in a three-layer cylindrical shell consisting of two isotropic layers of aluminum inside and outside the shell and a central layer of aluminum made of an auxetic cell structure of the re-internal honeycomb have been obtained. For this purpose, high-order shear deformation theory and the Galerkin numerical method are used. The assumed boundary conditions for the problem of simple support are considered on both sides of the shell. Finally, three parameters of length to radius (L/R), the ratio of the thickness of the auxetic core to the total thickness (h_c/h), and the cell angle of the auxetic structure's critical load are discussed. Based on the results, it can be stated:

- By increasing the ratio of length to radius (L/R), system stability and critical load decrease. As in all constant coefficients, L has the direct effect, and R has the opposite effect.
- The auxetic structure of the inner honeycomb is not stable in compressive loading, and with the increase of core thickness to total thickness ratio(h_c/h), the stability and load capacity decreases with a steep slope.
- Cell angle changes have a small effect on system stability. The explanation is that increasing the size of the cell angle *(θ)* increases the stiffness and stability of the system and will cause a small increase in the critical load of the system.

8- Nomenclature

A	Area, m^2
E	Modulus of Elasticity, N/m^2
$f_1(z)$	Considered different theories
$f_2(z)$	Considered different theories
G	Shear modulus, N/m^2
h	Total thickness of the shell
L	Length of shell
R	Rradius of shell
u_0	Longitudinal displacement of the middle plane
u_1	Longitudinal displacement
u_2	Circumferential displacement
u_3	Transverse displacement
U	Strain energy
v_0	Circumferential displacement of the middle plane

w_0	Transverse displacement of the middle plane
x, θ, z	Cylindrical-coordinate parameters
ν	Poisson's ratio
δ	The variation of the function
φ_1	Represent the rotation of the middle plane around the θ axis
φ_2	Represent the rotation of the middle plane around the x-axis

References

[1] T.J. Cui, D.R. Smith, R. Liu, Metamaterials, Springer, 2010.

[2] P.U. Kelkar, H.S. Kim, K.-H. Cho, J.Y. Kwak, C.-Y. Kang, H.-C. Song, Cellular auxetic structures for mechanical metamaterials: A review, Sensors, 20(11) (2020) 3132.

[3] M.S. Rad, H. Hatami, Z. Ahmad, A.K. Yasuri, Analytical solution and finite element approach to the dense re-entrant unit cells of auxetic structures, Acta Mechanica, 230 (2019) 2171-2185.

[4] L.J. Gibson, M.F. Ashby, G. Schajer, C. Robertson, The mechanics of two-dimensional cellular materials, Proceedings of the Royal Society of London. A. Mathematical and Physical Sciences, 382(1782) (1982) 25-42.

[5] A. Alderson, K. Alderson, Auxetic materials, Proceedings of the Institution of Mechanical Engineers, Part G: Journal of Aerospace Engineering, 221(4) (2007) 565-575.

[6] A. Pakrooyan, P. Yousefi, K. Khorshidi, M.M. Najafizadeh, A. Nezamabadi, Free vibration analysis of an auxetic honeycomb sandwich plate placed at the wall of a fluid tank, Ocean Engineering, 263 (2022) 112353.

[7] K. Khorshidi, M. Rezaeisaray, M. Karimi, Energy harvesting using vibrating honeycomb sandwich panels with auxetic core and carbon nanotube-reinforced face sheets, International Journal of Solids and Structures, 256 (2022) 111988.

[8] Y. Shabani, P. Mehdianfar, K. Khorshidi, Static buckling and free vibration analysis of bi-dimensional FG metal ceramic porous beam, Mechanics of Advanced Composite Structures, 11(1) (2024) 149-158.

[9] M. Amabili, M.P. Paı¨ doussis, Review of studies on geometrically nonlinear vibrations and dynamics of circular cylindrical shells and panels, with and without fluid-structure interaction, Appl. Mech. Rev., 56(4) (2003) 349-381.

[10] T. Von Karman, H.-S. Tsien, The buckling of thin cylindrical shells under axial compression, Journal of the Aeronautical Sciences, 8(8) (1941) 303-312.

[11] W. Baker, J. Bennett, C. Babcock, Experimental buckling investigation of ring-stiffened cylindrical shells under unsymmetrical axial loads, (1983).

[12] N. Yamaki, Elastic stability of circular cylindrical shells, Elsevier, 1984.

[13] C. Calladine, Understanding imperfection-sensitivity in the buckling of thin-walled shells, Thin-walled structures, 23(1-4) (1995) 215-235.

[14] E. Elishakoff, Y. Li, J.H. Starnes Jr, J. Cheney, Non-classical problems in the theory of elastic stability, Appl. Mech. Rev., 54(5) (2001) B86-B86.

[15] P.B. Gonçalves, Z.J. Del Prado, Nonlinear oscillations and stability of parametrically excited cylindrical shells, Meccanica, 37 (2002) 569-597.

[16] J.M.T. Thompson, Advances in shell buckling: Theory and experiments, International Journal of Bifurcation and Chaos, 25(01) (2015) 1530001.

[17] P. Kumar, C. Srinivasa, On buckling and free vibration studies of sandwich plates and cylindrical shells: A review, Journal of thermoplastic composite materials, 33(5) (2020) 673-724.

[18] A. Evkin, V. Krasovsky, O. Lykhachova, V. Marchenko, Local buckling of axially compressed cylindrical shells with different boundary conditions, Thin-Walled Structures, 141 (2019) 374-388.

[19] L.N. Ly, V.M. Duc, N.-T. Trung, N.T. Phuong, D.T. Dong, T.Q. Minh, N.V. Tien, V.T. Hung, An analytical approach to the nonlinear buckling behavior of axially compressed auxetic-core cylindrical shells with carbon nanotube-reinforced coatings, Proceedings of the Institution of Mechanical Engineers, Part L: Journal of Materials: Design and Applications, 235(10) (2021) 2254-2265.

[20] Y. Guo, J. Zhang, L. Chen, B. Du, H. Liu, L. Chen, W. Li, Y. Liu, Deformation behaviors and energy absorption of auxetic lattice cylindrical structures under axial crushing load, Aerospace Science and Technology, 98 (2020) 105662.

[21] K. Khorshidi, B. Soltannia, M. Karimi, M. Zakaryaei, Natural frequencies of submerged microplate structures, coupled to stationary fluid, using modified strain gradient theory, Composite Structures, 326 (2023) 117583.

[22] K. Khorshidi, M. Karimi, Analytical modeling for vibrating piezoelectric nanoplates in interaction with inviscid fluid using various modified plate theories, Ocean Engineering, 181 (2019) 267-280.

[23] K. Khorshidi, S. Savvafi, S. Zobeid, Forced vibration of a three-layer cylindrical shell with an auxetic core containing fluid under the influence of shock load using high-order shear deformation theories, Mechanic of Advanced and Smart Materials, 3(4) (2024) 431-464.

[24] K. Khorshidi, S. Savvafi, S. Zobeid, Investigation of

Free Vibration in Fluid-Loaded Cylindrical Shells with a Three-Layer Sandwich Wall and an Auxetic Central Layer, Mechanics of Advanced Composite Structures, (2024).

[25] M. Saeidiha, H. Ahmadi, A. Jalali, Nonlinear vibrations analysis of hyperelastic cylindrical shells utilizing the method of multiple scales, International Journal of Structural Stability and Dynamics, (2023) 2450209.

HOW TO CITE THIS ARTICLE

K. Khorshidi, S. Savvafi, S. Zobeid, Buckling Analysis of the Composite Sandwich Cylindrical Shell Integrated with Auxetic Metamaterial Core, AUT J. Mech Eng., 8(1) (2024) 31-42.

DOI: 10.22060/ajme.2024.23182.6110